British Journal of Cancer www.nature.com/bjc

ARTICLE

Translational Therapeutics

APC/*PIK3CA* mutations and β-catenin status predict tankyrase inhibitor sensitivity of patient-derived colorectal cancer cells

Mingjue Chen[1,2,10], Tetsuo Mashima[1,10], Taichi Oishi[1,2,10], Yukiko Muramatsu[1], Yosuke Seto[3], Manabu Takamatsu[4], Naomi Kawata[1,5], Shun Morino[1,2], Ayane Nakamura[1,6], Saori Inaba[1], Xunmei Yuan[1], Kohei Maruyama[2,3], Mai Suzuki[2,3], Ayana Sato[1,2], Haruka Yoshida[1], Myung-Kyu Jang[1,2], Anna Mizutani[1], Kengo Takeuchi[4], Kensei Yamaguchi[5], Fumiyuki Shirai[7], Satoshi Nagayama[8,9], Ryohei Katayama[2,3] and Hiroyuki Seimiya[1,2,6]✉

© The Author(s), under exclusive licence to Springer Nature Limited 2023

BACKGROUND: Aberrant WNT/β-catenin signaling drives carcinogenesis. Tankyrases poly(ADP-ribosyl)ate and destabilize AXINs, β-catenin repressors. Tankyrase inhibitors block WNT/β-catenin signaling and colorectal cancer (CRC) growth. We previously reported that 'short' *APC* mutations, lacking all seven β-catenin-binding 20-amino acid repeats (20-AARs), are potential predictive biomarkers for CRC cell sensitivity to tankyrase inhibitors. Meanwhile, 'Long' *APC* mutations, which possess more than one 20-AAR, do not predict inhibitor–resistant cells. Thus, additional biomarkers are needed to precisely predict the inhibitor sensitivity.
METHODS: Using 47 CRC patient-derived cells (PDCs), we examined correlations between the sensitivity to tankyrase inhibitors (G007-LK and RK-582), driver mutations, and the expressions of signaling factors. NOD.CB17-*Prkdc*^{scid}/J and BALB/c-nu/nu xenograft mice were treated with RK-582.
RESULTS: Short *APC* mutant CRC cells exhibited high/intermediate sensitivities to tankyrase inhibitors in vitro and in vivo. Active β-catenin levels correlated with inhibitor sensitivity in both short and long *APC* mutant PDCs. *PIK3CA* mutations, but not *KRAS*/*BRAF* mutations, were more frequent in inhibitor–resistant PDCs. Some wild-type *APC* PDCs showed inhibitor sensitivity in a β-catenin-independent manner.
CONCLUSIONS: *APC*/*PIK3CA* mutations and β-catenin predict the sensitivity of *APC*-mutated CRC PDCs to tankyrase inhibitors. These observations may help inform the strategy of patient selection in future clinical trials of tankyrase inhibitors.

British Journal of Cancer (2024) 130:151–162; https://doi.org/10.1038/s41416-023-02484-8

BACKGROUND

Colorectal cancer (CRC) is the third leading cause of cancer death worldwide. Currently, cytotoxic and targeted drugs and immune checkpoint inhibitors are used for the treatment of patients with unresectable advanced or recurrent CRC [1]. However, the efficacies of these approaches are limited. Therefore, new drugs are needed to improve patient outcome.

WNT/β-catenin signaling plays an important role in carcinogenesis. In approximately 80% of CRCs, loss-of-function mutations in *APC* tumor suppressor stabilize β-catenin and activate TCF/LEF-mediated gene transcription [2, 3]. Therefore, WNT/β-catenin signaling has been a rational therapeutic target for CRC.

Tankyrase poly(ADP-ribose) polymerase (PARP) regulates various cellular processes, including telomere maintenance, mitosis, and cell motility [4–6]. In CRC, tankyrase supports cell proliferation, enhancing WNT/β-catenin signaling by poly(ADP-ribosyl)ating AXINs, which are negative regulators of β-catenin, and targeting them for ubiquitin-dependent degradation [7–9]. Therefore, tankyrase is a potential therapeutic target for CRC [10, 11]. Various tankyrase inhibitors have been developed; these inhibitors cause AXIN accumulation and subsequent β-catenin degradation. Tankyrase inhibitors have been proven effective against CRC xenograft tumors [12–17]. However, developing tankyrase inhibitors as clinical drugs has remained challenging. First, not all *APC*-mutated CRC cells are sensitive to tankyrase inhibitors [13], and reliable biomarkers to predict drug sensitivity have not been established. Second, because WNT/β-catenin signaling regulates adult tissue homeostasis, such as intestinal stem cell maintenance, tankyrase inhibitors could meet a narrow therapeutic window [18], although recent two literatures have indicated that tankyrase inhibitors show antitumor efficacy without significant intestinal toxicity in mouse models [19, 20]. Therefore, it is important to

[1]Division of Molecular Biotherapy, Cancer Chemotherapy Center, Japanese Foundation for Cancer Research (JFCR), Tokyo, Japan. [2]Department of Computational Biology and Medical Sciences, Graduate School of Frontier Sciences, The University of Tokyo, Tokyo, Japan. [3]Division of Experimental Chemotherapy, Cancer Chemotherapy Center, JFCR, Tokyo, Japan. [4]Division of Pathology, The Cancer Institute, JFCR, Tokyo, Japan. [5]Gastroenterological Chemotherapy, Cancer Institute Hospital, JFCR, Tokyo, Japan. [6]Graduate School of Pharmaceutical Sciences, Meiji Pharmaceutical University, Tokyo, Japan. [7]Drug Discovery Chemistry Platform Unit, RIKEN Center for Sustainable Resource Science, Saitama, Japan. [8]Gastroenterological Surgery, Cancer Institute Hospital, JFCR, Tokyo, Japan. [9]Department of Surgery, Uji-Tokushukai Medical Center, Kyoto, Japan. [10]These authors contributed equally: Mingjue Chen, Tetsuo Mashima, Taichi Oishi. ✉email: hseimiya@jfcr.or.jp

Received: 11 December 2022 Revised: 24 October 2023 Accepted: 27 October 2023
Published online: 15 November 2023

identify predictive biomarkers for the response to tankyrase inhibitors.

In APC protein, seven 20 amino acid repeats (20-AARs) play a central role for β-catenin binding and degradation. We previously demonstrated that CRC cell lines with truncation mutations in *APC* that encodes a mutant protein lacking all the seven 20-AARs (hereafter referred to as 'short APC') were sensitive to tankyrase inhibitors [21]. In CRC cells derived from a small cohort of patients, the short *APC* type cells were sensitive to tankyrase inhibitors. However, some 'long *APC*' type patient-derived cells (PDCs), which possess more than one 20-AAR, were also sensitive to tankyrase inhibitors. Thus, long *APC* mutations cannot be an exclusion criterion for tankyrase inhibitor sensitivity. Therefore, investigating other biomarkers for drug sensitivity is required.

Here, using an expanded panel of 47 CRC PDCs, we evaluated the correlation of sensitivity to tankyrase inhibitors with CRC driver mutations. We also examined the expression levels and responses of the related signaling factors.

METHODS

Chemical compounds

RK-582 was synthesized as described previously [16]. G007-LK, BKM-120 and trametinib were purchased from Selleck Chemicals (Houston, TX, USA).

Cell culture and proliferation assay

CRC PDCs were established with approval from an institutional review board of Japanese Foundation for Cancer Research and the written informed consent of patients [21]. The cells were maintained in StemPro ESC medium (Thermo Fisher Scientific, Waltham, MA, USA) supplemented with 10 μM Y-27632 (Nacalai Tesque, Kyoto, Japan) and Antibiotic-Antimycotic Solution (Thermo Fisher Scientific) [21]. SW480 cells were purchased from American Type Culture Collection (Manassas, VA, USA). Kato III cells were obtained from Cell Resource Center for Biomedical Research, Tohoku University (Miyagi, Japan). These cells were maintained in RPMI-1640 medium (Gibco, Life Technologies, Paisley, UK) supplemented with 10% fetal bovine serum, and authenticated by short tandem repeat profiling analysis (BEX, Tokyo, Japan) before the experiments. Cells were routinely tested for mycoplasma contamination by PCR with the primers 5′-CACCATCTGTCACTCTGTTAACC-3′ and 5′-GGAGCAAACAGGATTAGATACCC-3′. Cell proliferation was evaluated using thiazolyl blue tetrazolium bromide (Sigma, St Louis, MO, USA), as previously described [22]. Depending on the drug sensitivity, cells were classified in three categories, sensitive, intermediate, and resistant as follows: cells were defined as sensitive if the average of relative cell numbers upon treatment with 0.33 to 3 μM G007-LK were ≤70%; intermediate if >70% and ≤80%; and resistant if over 80%. Experiments were repeated at least twice.

Genetic analysis of mutation status

Raw next-generation sequencing (NGS) reads were initially preprocessed by removing Illumine adapter sequences and low-quality bases using Trimmomatic-0.38 [23] with LEADING:20 TRAILING:20 SLIDINGWINDOW:4:30 MINLEN:40. The quality-controlled paired-end NGS reads were aligned against the UCSC hg38 human genome sequence by BWA-MEM [24], and the obtained SAM file was converted to a BAM file by SAMtools v1.8 [25]. Somatic mutations were detected using Mutect2 implemented in GATK v4 [26, 27] by comparing tumor and matched normal sample data. In this process, we conducted base quality score recalibration (BQSR) and filtering of ambiguous mutations in accordance with the GATK best practices workflows [28, 29]. Detected mutations were annotated by Variant Effect Predictor (VEP) [30]. For the mutation call of *APC* gene, we set up ≥5% variant allele frequency as cut-off value. As for the *APC* mutation status, we also confirmed all the mutation in patient-derived cells (PDCs) by Sanger method, as described previously [21].

Immunoblot analysis

Immunoblotting was performed as previously described [22]. The antibodies used are listed in Supplementary Table 1. Signals were quantitated using ImageJ software. Experiments were repeated at least twice. The amount of loaded protein in each sample was confirmed by staining membranes with 2% Ponceau-S/ 5% acetic acid solution (all the data were shown in Supplementary Fig. 1).

Immunofluorescence staining

Cells on collagen-coated 96-well plates were fixed with 2% formaldehyde/phosphate-buffered saline (PBS) and permeabilized with 0.5% Nonidet P-40/PBS. Immunofluorescence staining was performed as previously described [21] with rabbit anti-non-phosphorylated (active) β-catenin (Ser33/37/Thr41) (D13A1, Cell Signaling Technology, Danvers, MA, USA). Nuclei were counterstained with VECTASHIELD antifade mounting medium with 4′,6-dia-midino-2-phenylindole (DAPI; Vector Laboratories, Newark, CA, USA). Images were captured using IX-71 (Olympus, Tokyo, Japan) or INCELL Analyzer 6000 (GE Healthcare Life Sciences, Marlborough, MA, USA). Nuclear active β-catenin levels were quantified using Developer Toolbox1.9.2 (GE Healthcare Life Sciences). Experiments were repeated at least twice.

Xenograft mouse experiments

All animal procedures were carried out in the animal experiment room at the Japanese Foundation for Cancer Research (JFCR) according to protocols approved by the JFCR Animal Care and Use Committee. COLO-320DM cells were suspended in Matrigel (Corning, Corning, NY, USA) and HBSS in a 1:1 ratio (5.2×10^6 cells/100 μL/mouse) and were implanted subcutaneously in the rear right flank of 6-week-old female NOD.CB17-*Prkdc*^{scid}/J mice (Charles River Laboratories Japan, Inc., Kanagawa, Japan). The length (L) and width (W) of the tumor mass were measured, and the tumor volume (TV) was calculated using the equation: $TV = (L \times W^2)/2$. When tumor volumes reached approximately 100 mm^3, mice were randomly separated into groups of 10 animals with similarly sized tumors on average, and treatment with either vehicle, 5 mg/kg or 20 mg/kg RK-582 was initiated on the same day of grouping. The sample size was determined based on our previous experiments [15, 16]. For intraperitoneal administration, dosing solution contained 15% DMSO, 17.5% Cremophor, 8.75% ethanol, 8.75% PEG-40 hydrogenated castor oil and 50% PBS. Pharmacodynamic analysis was carried out with immunoblotting as described above. Experiments with COLO-320DM xenograft tumors were repeated with slight modifications three times. HCT-15 cells were suspended in Matrigel and HBSS in a 1:1 ratio (5×10^6 cells/100 μL/mouse) and were implanted subcutaneously in the rear right flank of 5-week-old female BALB/c-nu/nu mice (Charles River Laboratories Japan, Inc). When tumor volumes reached approximately 200 mm^3, mice were randomly separated into groups of 6 animals with similarly sized tumors on average, and treatment with vehicle or 20 mg/kg RK-582 was initiated on the same day of grouping. Other detailed conditions and procedures are described in Supplementary Methods.

Immunohistochemistry

The original cases for developing PDCs (JC-32, 35, 73, 79, 110, 288, 462, and 475 cells for tankyrase inhibitor-sensitive cells and JC-9, 33, 47, 55, 61, 63, 119, and 175 cells for resistant cells, respectively) were histologically evaluated. Serial 5-mm thick tissue sections of the whole lesion were cut from resected specimens fixed with 20% buffered formalin, and embedded in paraffin, and then 4-μm thick sections were prepared for staining. For each case, representative sections including the largest tumor component were selected by histologic assessment on hematoxylin-eosin (H&E) staining. The sections were applied for immunohistochemistry with following two antibodies: mouse monoclonal anti-β-catenin, clone: 14/Beta-Catenin (1:3,000, BD Transduction Laboratories, Franklin Lakes, NJ, USA); rabbit monoclonal anti-active (non-phospho)-β-Catenin, clone: D2U8Y (1:2,000, Cell Signaling Technology). The staining procedures were performed using an auto-stainer (Leica Bond-III, Leica Biosystems). The percentage of the positive staining areas for tumor nuclei were evaluated by pathologist (MT).

Transcriptome analysis

Total RNA was extracted from JC-11, 21, 475, and JC-494 cells using a Fast Gene RNA Basic kit (Nippon Genetics, Tokyo, Japan) and quantified using the Agilent 2100 Bioanalyzer (Agilent Technologies, Santa Clara, CA, USA). cDNA microarray analysis was performed using the GeneChip Human Genome U133 Plus 2.0 Array (Thermo Fisher Scientific). Data normalization was performed using GeneSpring GX software (Agilent Technologies). Gene set enrichment analysis (GSEA) (Broad Institute, Cambridge, MA, USA) was performed on the website (http://software.broadinstitute.org/gsea/

index.jsp). The gene expression data have been deposited in the Gene Expression Omnibus (accession number GSE217758 and GSE232209).

Reverse transcription-quantitative PCR (RT-qPCR)

RNA was extracted as described above, and cDNA was synthesized using SuperScript III First-Strand Synthesis SuperMix for RT-qPCR (Life Technologies, Carlsbad, CA, USA). qPCR was done by a LightCycler 96 (Roche, Basel, Switzerland). Primer sequences were as follows: *c-myc* forward primer: 5′-GCTGCTTAGACGCTGGATTT-3′, *c-myc* reverse primer: 5′-TAACGTTGAGGGCATCG-3′.

Small interfering RNA (siRNA) transfection

Silencer Select siRNAs for *SMYD2* [s32469(#1) and s32470(#2)], *CDKN1A* (p21) [s415(#1), s416(#2), and s417(#3)], *CTNNB1* (β-catenin) [s438] and negative control siRNAs were purchased from Thermo Fisher Scientific. siRNAs were transfected into cells using the Neon Transfection System (Thermo Fisher Scientific) as previously described [21]. Experiments were repeated twice.

Statistical analysis

Statistical significance was evaluated by Welch's *t*-test (when normality but not equal variance was assumed) or Mann–Whitney test (when normality was not assumed). For multi-group comparison, we used one-way analysis of variance (ANOVA) followed by Tukey–Kramer post-hoc test (when normality was assumed) or Kruskal–Wallis test (when normality was not assumed). These analyses were done by GraphPad Prism (version 8 and 9). For the experiments with multiple repeated measures, statistical significance was evaluated by repeated ANOVA using Microsoft Excel with Statcel 4 software.

RESULTS

Short APC as a biomarker for tankyrase inhibitor–sensitive CRC cells

Our previous analysis with 16 *APC*-mutated CRC PDCs showed the short APC mutations as a potential biomarker for sensitivity to tankyrase inhibitors [21]. To validate this observation, we analyzed additional 26 *APC*-mutated CRC PDCs. As shown in Fig. 1a, the PDCs were classified into three categories: sensitive, intermediate, and resistant to tankyrase inhibitors (G007-LK and RK-582), using previously defined criteria [21]. The sensitivity patterns were highly similar between these two structurally distinct inhibitors [13, 16] (Fig. 1b), excluding the possibility that the growth inhibition was caused through their off-target effects.

Genetic analysis (Table 1, Supplementary Table 2) revealed that all the short *APC* PDCs (16 out of 16) exhibited high/intermediate sensitivities to the tankyrase inhibitors, whereas the long *APC* PDCs were sensitive/intermediate (16 samples) and resistant (10 samples) (Fig. 1c). In short *APC* PDCs, such as JC-21 and JC-73, G007-LK and RK-582 caused AXIN2 accumulation and decreased the levels of active β-catenin (Fig. 1d). Though *AXIN2* is transcriptionally controlled downstream of β-catenin [13], tankyrase inhibitor treatment continuously caused AXIN2 protein accumulation and the decrease of active β-catenin even after longer exposure of the agents (Supplementary Fig. 2). By contrast, in JC-63, a tankyrase inhibitor–resistant long *APC* PDC, basal active β-catenin level was low. We also examined APC protein expression in these PDCs. The data confirmed that the APC protein size corresponded to the mutation status of *APC* gene in more than half of the PDCs, while there were several PDCs that expressed APC proteins with unexpected sizes (Supplementary Fig. 3).

We performed xenograft mouse model experiments with CRC COLO-320DM and HCT-15 cell lines, which are classified into short and long APC types, respectively. While COLO-320DM cells are sensitive to tankyrase inhibitors, including RK-582, HCT-15 cells are resistant to the inhibitors in culture [16, 21]. Consistent with such data, RK-582 exhibited dose-dependent antitumor effects on COLO-320DM but not HCT-15 xenograft tumors under tolerable dosing in vivo (Supplementary Fig. 4). Pharmacodynamic evaluation of AXIN2 accumulation in both xenograft tumors confirmed that RK-582 sufficiently inhibited tankyrase enzymes in the tumors. These observations support that short APC type CRC cancer cells are susceptible to the deleterious effect of tankyrase inhibitors even in vivo. Meanwhile, we tried to establish the patient-derived xenograft (PDX) models by using representative PDCs. However, efficiencies of the tumor formation and growth rates of the resulting tumors, if any, were too low to perform extensive therapeutic experiments.

Active β-catenin predicts cell sensitivity to tankyrase inhibitors

Because tankyrase inhibitors block CRC cell growth by degrading β-catenin [8, 31], we monitored the expression levels of WNT/β-catenin pathway proteins. In the initial analysis of 16 *APC*-mutated PDCs, the tankyrase inhibitor–sensitive cells expressed higher levels of active β-catenin compared with the intermediate/resistant cells (Fig. 2a). Tankyrase inhibitor–sensitive cells expressed active β-catenin either at higher levels or in nuclei, while nuclear active β-catenin levels were low in the resistant cells (Fig. 2b and Supplementary Fig. 5). Further analysis of 42 cases, including the above-mentioned 16 and additional 26 PDCs, demonstrated that the levels of active β-catenin correlated with the sensitivity to G007-LK and RK-582 (Fig. 2c–e). Importantly, we observed similar results with long *APC* type PDCs (Fig. 2f–h) and found that PDCs with mutant APC shorter than 1400 amino acids (aa) expressed higher levels of active β-catenin than those with mutant APC longer than 1400 aa (Fig. 2i). These observations indicate that active β-catenin may serve as a predictive biomarker of tankyrase inhibitor–sensitive cells. We further tested the effect of β-catenin knockdown (Supplementary Fig. 6A) and found that β-catenin knockdown preferentially suppressed the proliferation of the tankyrase inhibitor-sensitive PDCs (Supplementary Fig. 6B, C). These data provide additional proof that the colorectal cancer cells with highly active β-catenin could be preferentially dependent their growth on WNT/β-catenin signaling.

To confirm the correlation of tankyrase inhibitor sensitivity with WNT/β-catenin activity further, we examined total and active β-catenin levels in the original tumor tissues of the PDCs. As shown in Fig. 3, significantly higher nuclear total and active β-catenin levels were observed in the tissues from which the tankyrase inhibitor-sensitive PDCs were derived. These data indicate that our results with the PDCs would reflect the WNT/β-catenin activation status in clinical settings.

β-catenin functions as a transcriptional regulator in the nucleus [32]. Overall, tankyrase inhibitor–sensitive PDCs expressed higher levels of nuclear active β-catenin (Supplementary Fig. 7A, B). Nuclear localization of β-catenin is regulated by SMYD2, an N-lysine methyltransferase [33]. We found that the amounts of SMYD2 positively correlated with those of nuclear active β-catenin (Supplementary Fig. 7C, D). In a tankyrase inhibitor–sensitive, short *APC* type PDC (JC-39), SMYD2 depletion (Supplementary Fig. 8A) decreased nuclear active β-catenin (Supplementary Fig. 8B). These observations suggest that SMYD2 regulates the nuclear localization of β-catenin, which promotes the proliferation of tankyrase inhibitor–sensitive CRCs.

PIK3CA mutations but not *KRAS*/*BRAF* mutations are associated with sensitivities to tankyrase inhibitors in *APC*-mutated CRC cells

We next examined the genetic status of major CRC driver genes (Table 1). We observed significantly high levels of *PIK3CA* mutations in the inhibitor–resistant cells (Supplementary Table 3 and Fig. 4a). By contrast, there was no significant relationship between drug sensitivity and *KRAS*, *BRAF*, and *TP53* mutations. We further examined AKT and extracellular signal-regulated kinase (ERK) phosphorylation (i.e., activation) (Supplementary Fig. 9A) and found that the levels of AKT phosphorylated at Ser-473

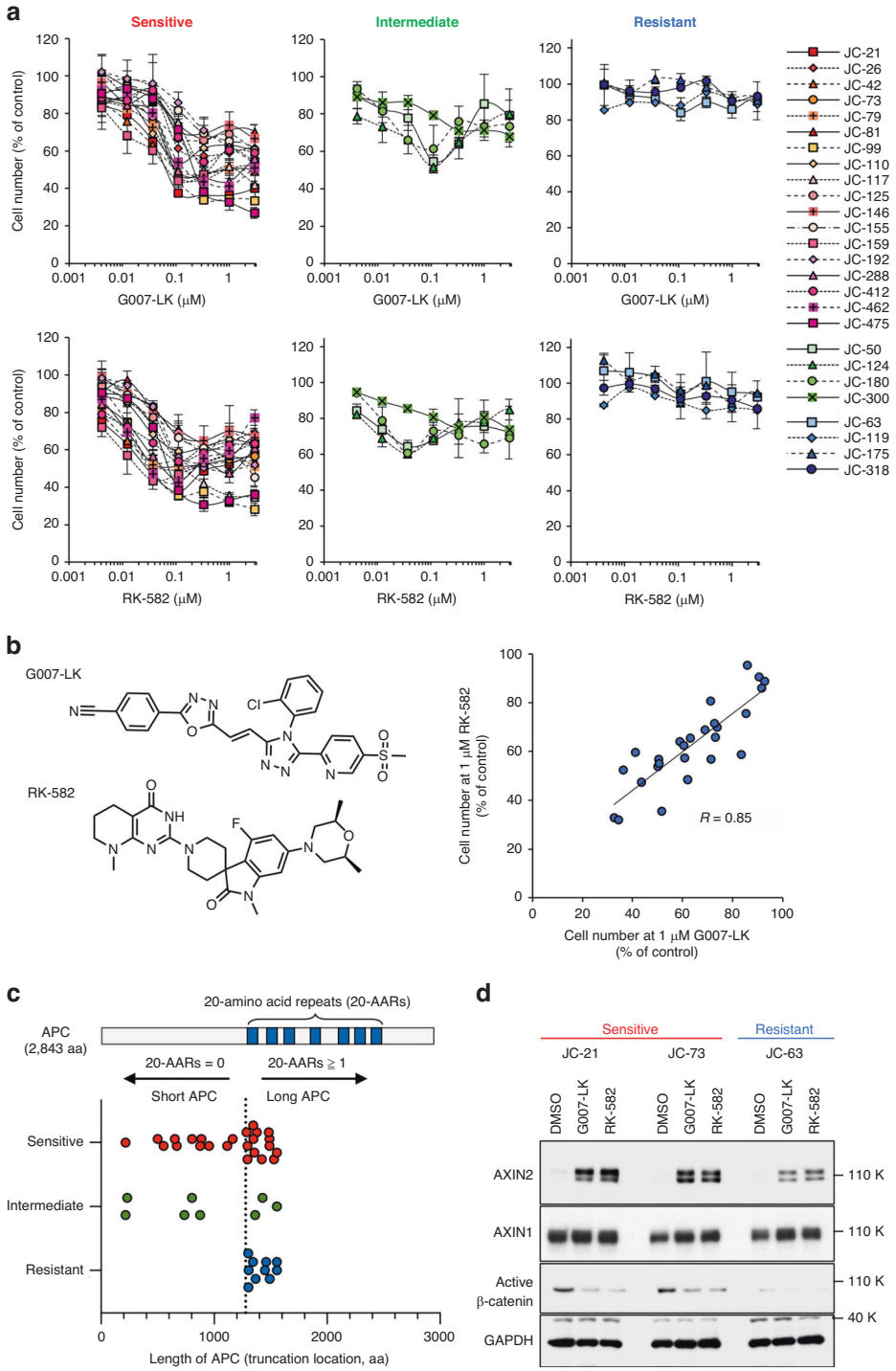

Fig. 1 Colorectal cancer (CRC) patient-derived cells (PDCs) with 'short' APC mutations are sensitive to tankyrase inhibitors. a Cell viability of CRC PDCs (expanded cohort with 26 patients) was evaluated by thiazolyl blue tetrazolium bromide (MTT) assay after 5-day treatment with tankyrase inhibitors, G007-LK and RK-582, at indicated doses in triplicate. Experiments were repeated at least twice, and the average values were plotted. *Error bar* indicates standard deviation. Depending on their sensitivity, cells were classified in three categories, sensitive, intermediate and resistant, using criteria as described in Methods. **b** Correlation of PDC sensitivities to G007-LK and RK-582. Structures of G007-LK and RK-582 (*left*). Relative cell numbers upon 5-day treatment with 1 μM of the inhibitors were plotted [data were derived from (**a**)] (*right*). *R*: Pearson's correlation score. **c** Correlation between APC length (truncated point) and sensitivity to G007-LK in the 42 CRC PDCs, including the initial and expanded cohorts of 16 and 26 patients, respectively, is shown by dot plot. Dotted line indicates the border of the short and long APC mutants. 20-AAR: 20-amino acid repeat, aa: amino acid. **d** Effect of tankyrase inhibitors on the protein levels of WNT/β-catenin pathway regulators in the inhibitor-sensitive and -resistant CRC PDCs. Cells were treated with G007-LK and RK-582 (0.3 μM) for 24 h and immunoblotting was performed. Glyceraldehyde-3-phosphate dehydrogenase (GAPDH) expression served as a loading control. For (**a**–**c**), each experiment was performed at least twice, and reproducible results were obtained. For (**d**), experiments were performed twice, and reproducible results were obtained.

Table 1. Mutation status of typical cancer driver genes in colorectal cancer patient–derived cells.

JC-	*APC* truncation point	*KRAS*	*BRAF*	*PIK3CA*	*TP53*
7	R232X	WT	WT	WT	R273C
9	WT	WT	V600E	WT	R156H
11	WT	WT	V600E	R357Q	R175H
20	P1483fs	G13D	WT	WT	M2371
21	Q886X	WT	WT	WT	R306X
26	S1347X	WT	WT	WT	WT
32	W553X	WT	WT	WT	C141Y
33	Q1303X	A146T	WT	H1047R	R273C, A138V
35	I1164fs	WT	WT	WT	WT
36	R805X	A146T	WT	K111N, R398H	WT
37	T1556fs	WT	WT	E545K	R175H
39	R216X	G13D	WT	WT	WT
42	S1356X	G13D	WT	WT	WT
47	F1491fs	G12V	WT	H1047R	R248W
49	R302X, E1345X	WT	WT	WT	C238fs
50	K736Sfs*25	V7L	WT	WT	L264Yfs*81
52	L1342X, S1343fs	WT	WT	WT	R213X
54	R876X	G12D	WT	WT	R273H
55	E1306X	A146T	WT	N1044K	M246K
56	T1023fs, E1554X	G12D	WT	WT	WT
58	E1295X	WT	WT	H1047R	R158H
61	E941X, T1459fs	G12D	WT	N1044K	WT
63	Q1367X	WT	WT	WT	Y220C
69	WT	WT	WT	WT	S166X
73	R499X	WT	WT	WT	H179dup
79	R876X	G12V	WT	WT	R282W
81	L1489X	G12V	WT	WT	S241F
99	Q1378X	WT	WT	WT	R175H
110	L954X	WT	WT	WT	R273H
117	I1287Rfs*3	G12D	WT	WT	WT
119	L1302Rfs*3	G13D	WT	WT	P152Rfs
124	S1362Kfs*52	Q61L	WT	WT	G266R
125	G1116Efs*6	WT	WT	WT	W53X
146	K670X	G12V	WT	WT	R196*
155	Y935X, L1489Yfs*18	G12V	WT	WT	WT
159	S1421Rfs*52	G12S	WT	WT	E171X
175	L665Ifs*8, R1450X	G12S	WT	WT	R175H
180	R216X	WT	WT	WT	WT
192	E633X, E1494X, Q1529X	WT	V600E	WT	E286K
215	WT	WT	V600E	R93W	R175H
288	S299Tfs*7, R805X	G12C	WT	WT	P151S
300	Q264X, Q1429X	G12D	WT	WT	Y220C
318	V830Gfs*12, T1556Nfs*3	WT	V600E	E542K	W53X
412	S1465Wfs*3, T1556Nfs*3	WT	V600E, D565A	R108C	WT
462	R499X, E1295X	WT	WT	WT	Q192X
475	R653K[a]	G12C	WT	WT	M246L
494	WT	WT	V600E	WT	WT

All the *APC* sequence data were derived from the cultured cells.
"fs" means flameshift mutation. For example, "K736Sfs*25" means that lysine 736 is altered to serine, starting with which the 25th is a termination codon.
[a]The next exon is skipped because of this mutation, causing frameshift from this sequence.

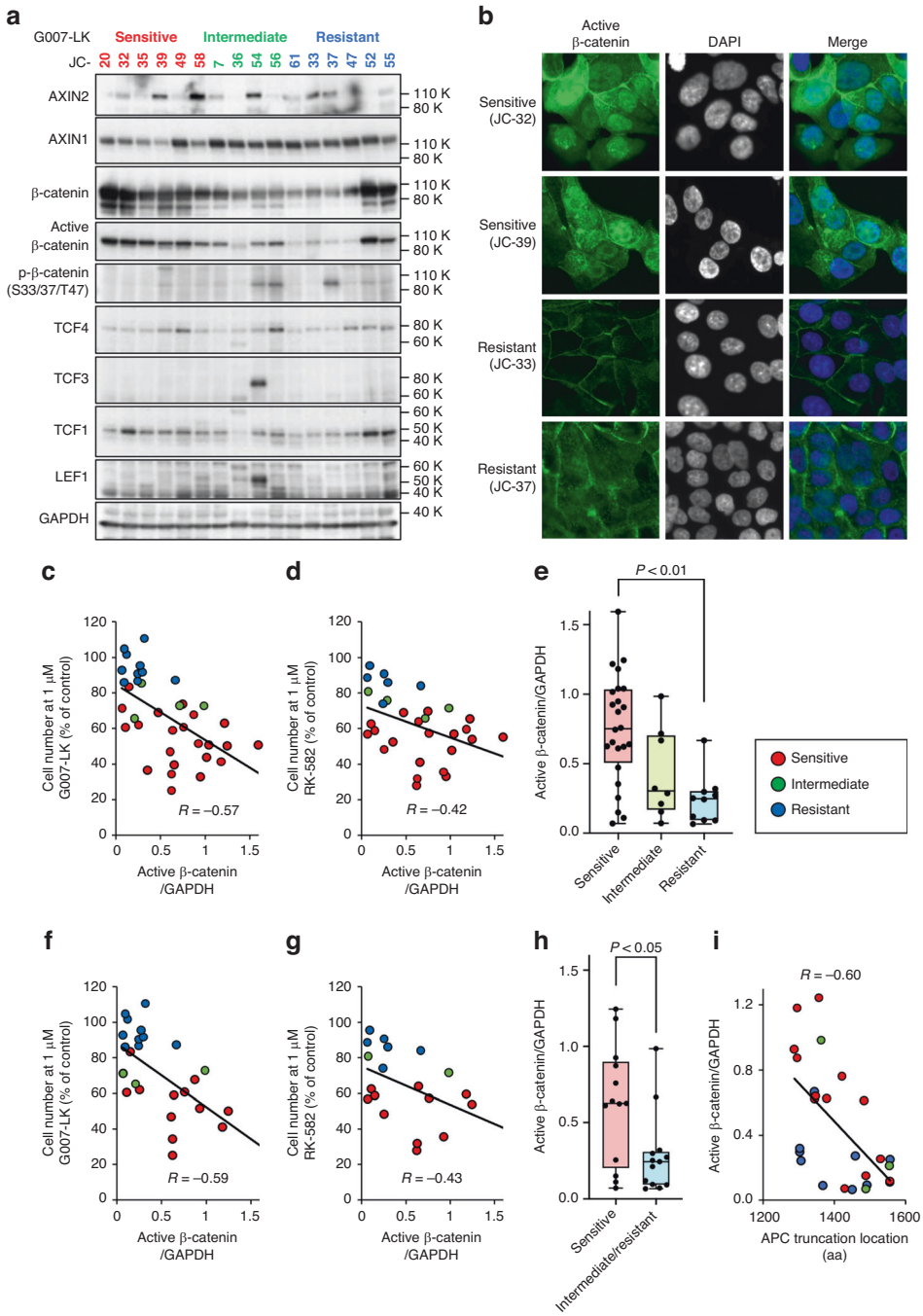

Fig. 2 Active β-catenin level marks tankyrase inhibitor-sensitive cells in the CRC PDCs with 'long' APC mutations. a Expression of the WNT/β-catenin axis proteins in CRC PDCs (initial cohort of 16 APC-mutated cell samples) examined by immunoblot analysis. GAPDH expression served as loading control. The numbers on the top of the blot represent the cell identification. **b** Immunofluorescence staining of active (non-phosphorylated) β-catenin in CRC PDCs. Cells were fixed and stained with anti-non-phosphorylated (at Ser33/37/Thr41) β-catenin antibody. Nuclei were counterstained with 4′,6-diamidino-2-phenylindole (DAPI). Representative data of tankyrase inhibitor–sensitive (JC-32, JC-39) and –resistant (JC-33, JC-37) cells are shown; data for other cells are shown in Supplementary Fig. 5. **c**, **d** Correlation between sensitivity to tankyrase inhibitors [G007-LK (**c**) or RK-582 (**d**)] and active β-catenin level quantitated by immunoblot analysis in the combined cohort (**c**) and in the expanded cohort (**d**). *R*: Pearson's correlation score. **e** Expression levels of active β-catenin protein in the CRC PDCs based on G007-LK sensitivity. *Error bars* indicate the minimum and maximum values. **f**, **g** Correlation between sensitivity to G007-LK (**f**) or RK-582 (**g**) and active β-catenin level in the long APC-type PDCs of the combined cohort (**f**) and expanded cohort (**g**). **h** Expression levels of active β-catenin in the long APC-type CRC PDCs based on G007-LK sensitivity. In this graph, intermediate and resistant PDCs were merged because the number of the intermediate group was too small. *Error bars* indicate the minimum and maximum values. **i** Correlation between active β-catenin level and APC length (truncated point) in the long APC-type PDCs. For (**a**), experiments were performed twice, and reproducible results were obtained. For other data, each experiment was performed at least twice, and reproducible results were obtained. For (**e**, **h**), statistical significance was evaluated by Kruskal–Wallis and two-sided Mann–Whitney tests, respectively (since normality was not assumed), using GraphPad Prism (version 9).

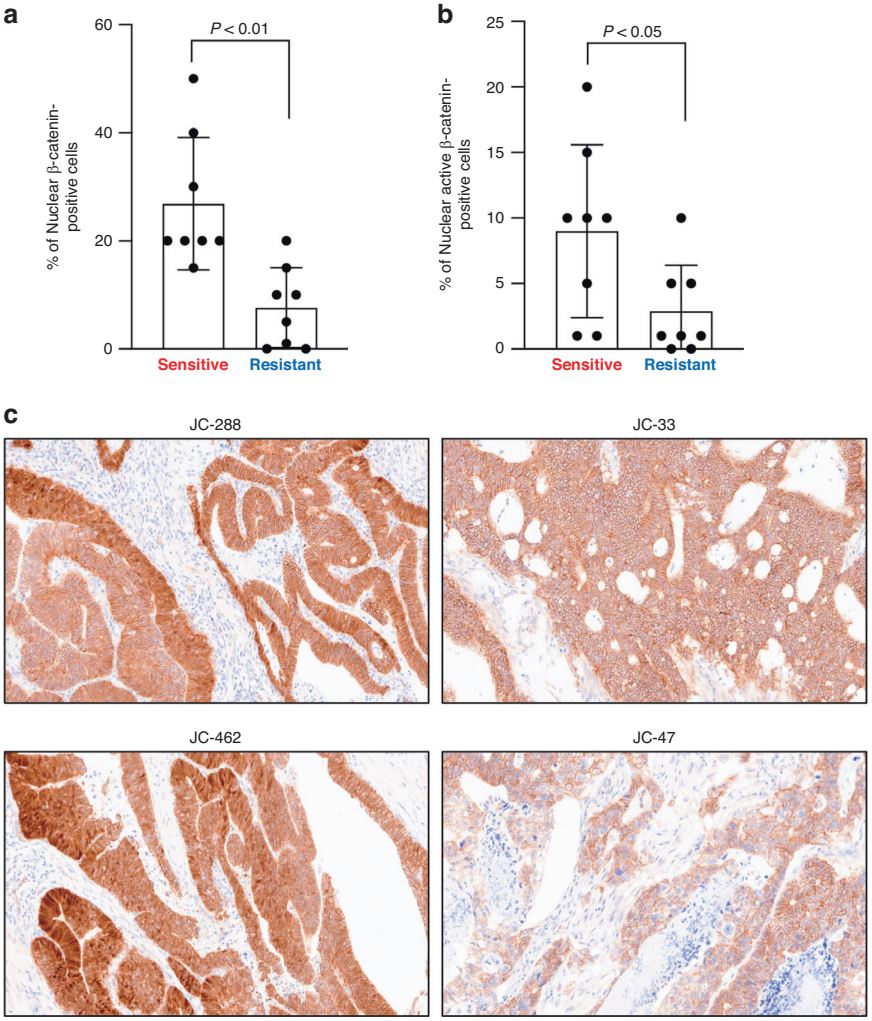

Fig. 3 Tankyrase inhibitor sensitivity in the CRC PDCs correlates with β-catenin activation status in the original tumor tissues. **a**, **b** Histological evaluation of the β-catenin activation status in the original CRC tissues from which PDCs were derived (JC-32, 35, 73, 79, 110, 288, 462, and 475 cells for tankyrase inhibitor-sensitive cells and JC-9, 33, 47, 55, 61, 63, 119, and 175 cells for resistant cells, respectively). The sections were stained with mouse monoclonal anti-β-catenin, clone: 14/Beta-Catenin for total β-catenin and with anti-rabbit monoclonal anti-non-phospho-β-catenin, clone: D2U8Y for active β-catenin. To evaluate the percentage of nuclear total (**a**, **b**) active β-catenin-positive cells, the positive staining areas for tumor nuclei were evaluated. Statistical significance was evaluated by two-sided Mann-Whitney test (since normality was not assumed) using GraphPad Prism (version 8). *Error bar* indicates standard deviation. **c** Representative data of active β-catenin staining for tankyrase inhibitor–sensitive (JC-288, JC-462) and –resistant (JC-33, JC-47) cells.

(phospho-AKT) tend to be higher in *PIK3CA* mutant cells than the wild-type cells among *APC*-mutated PDCs although *PIK3CA* mutations were not necessarily associated with high phospho-AKT levels (Fig. 4b). Phospho-AKT levels corelated with G007-LK sensitivity in *APC* mutated PDCs and in all the PDCs, to a lesser extent (Supplementary Fig. 9B). In contrast, ERK phosphorylated at Thr-202/Tyr-204 (phospho-ERK) was widely detected in PDCs regardless of tankyrase inhibitor sensitivity (Supplementary Fig. 9A). These results suggest that the phosphatidylinositol-3 kinase (PI3K)-AKT pathway is associated with the resistance to tankyrase inhibitors.

To determine the involvement of the PI3K-AKT pathway in tankyrase inhibitor resistance, we examined the combinational effect of G007-LK with a PI3K inhibitor, BKM-120, in the PDCs with high phospho-AKT. BKM-120 decreased the level of phospho-AKT in JC-54 in a dose-dependent manner, whereas it had no effect in JC-61 cells (Supplementary Fig. 10A). G007-LK and BKM-120 had an additive effect on JC-54 cell growth (Supplementary Fig. 10B).

We also examined the combinational effect of G007-LK with a MAPK/ERK kinase (MEK) inhibitor, trametinib, on phospho-ERK-positive PDCs. Under the conditions in which phospho-ERK was decreased (Supplementary Fig. 10C), G007-LK enhanced the growth inhibitory effect of trametinib on JC-39, JC-49, and JC-61 (Supplementary Fig. 10D). In CRC SW480 cells, the MEK inhibitor selumetinib upregulates fibroblast growth factor receptor 2 (FGFR2), and tankyrase inhibition attenuates this FGFR2 upregulation [34]. Using trametinib and G007-LK, we reproduced these results in SW480 cells (Supplementary Fig. 10E). In our PDCs, however, FGFR2 was not induced by trametinib. These observations indicate that tankyrase inhibitors can enhance the anti-proliferative effect of MEK inhibitors even in an FGFR2-independent manner.

Tankyrase inhibitors affect wild-type *APC* CRC cells

While tankyrase enhances WNT/β-catenin signaling, it also regulates other signaling pathways [4–6, 10]. We analyzed wild-type *APC* CRC PDCs (*APC*-wild cells) and identified two (out of five) cell lines, JC-11 and JC-494, that were highly sensitive to G007-LK and RK-582 (GI50 values for G007-LK were less than 1 μM, and those for RK-582 were less than 0.1 μM) (Fig. 5a). Meanwhile, JC-69

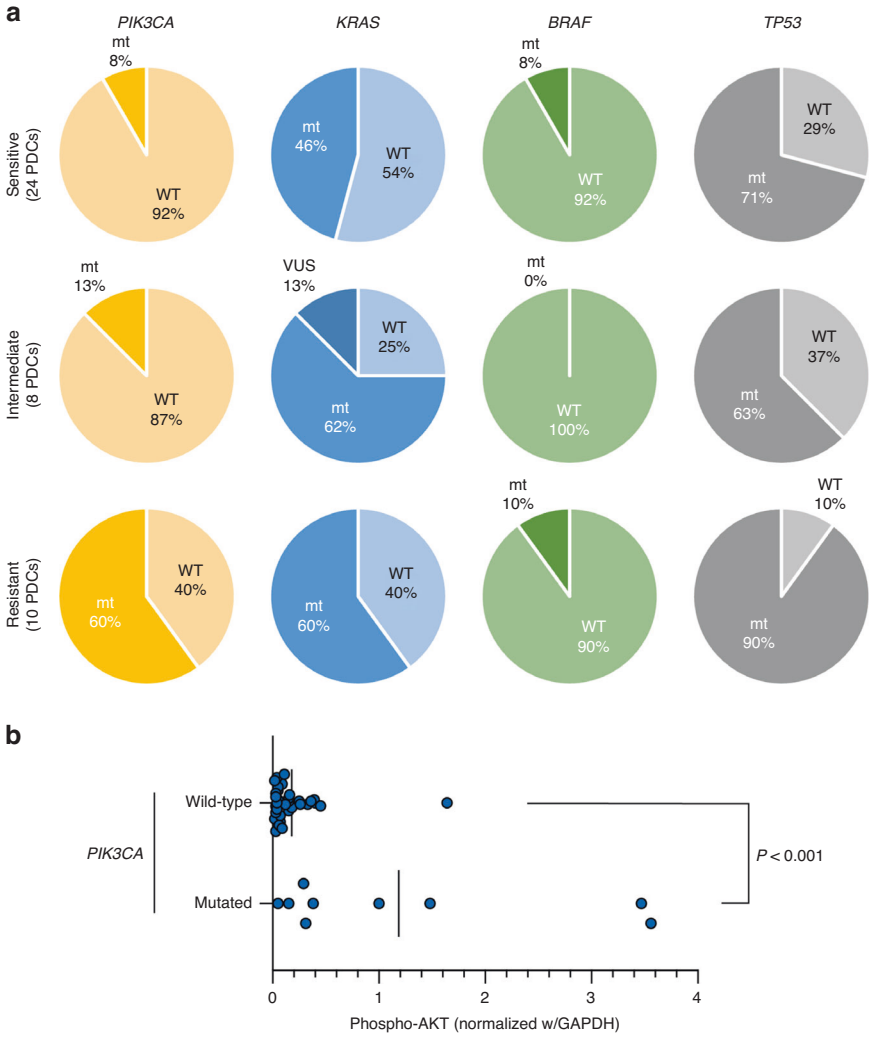

Fig. 4 Frequency of oncogenic driver mutations in the tankyrase inhibitor–responsive and –resistant CRC PDCs with APC mutations. **a** Comparison of *PIK3CA*, *KRAS*, *BRAF*, and *TP53* mutation frequencies between the tankyrase inhibitor (G007-LK)-responsive (sensitive/intermediate) and -resistant PDCs. Pie charts were drawn on the bases of data in Table 1. **b** Correlation between phosphorylated (active) AKT level and *PIK3CA* mutation status in the CRC PDCs, including the initial (16 patients) and expanded (26 patients) cohorts. Active AKT levels normalized by GAPDH expression were quantified from immunoblot data (Supplementary Fig. 9). Each experiment was performed twice, and reproducible results were obtained. Statistical significance was evaluated by two-sided Mann–Whitney test (since normality was not assumed) using GraphPad Prism (version 8).

exhibited a weaker sensitivity to the inhibitors (GI50 values for G007-LK were greater than 1 μM, and those for RK-582 were greater than 0.1 μM). Therefore, we focused on JC-11 and JC-494 for further analyses, which expressed only marginal amounts of active β-catenin (Supplementary Fig. 11A) and low amounts of β-catenin target genes (Supplementary Fig. 11B, *left*). In JC-11 and JC-494, tankyrase inhibitors did not significantly reduce β-catenin levels (Fig. 5b) or β-catenin target gene expression [35] (Supplementary Fig. 11B, *right*), suggesting a WNT/β-catenin-independent effect. Intriguingly, while tankyrase inhibitors caused accumulation of AXIN2 in *APC*-mutated PDCs (Fig. 1d), these *APC*-wild PDCs exhibited accumulation of AXIN1 but not AXIN2 upon the inhibitor treatment (Fig. 5b). Among other three wild-type APC PDCs, JC-9 and JC-69 showed low active β-catenin levels, whereas JC-215 expressed high level (Supplementary Fig. 11A). In JC-215 cells, we detected mutations both in *RNF43* (659 fs) and *ZNRP3* (R245X) genes, which would lead to β-catenin activation.

Tankyrase inhibitors also target YAP, PI3K/AKT, and MYC pathways [35]. In the *APC*-wild PDCs, tankyrase inhibitors did not affect phospho-AKT or phospho-ERK (Supplementary Fig. 11C). Moreover, tankyrase inhibitors did not affect YAP [36] signature gene expression (Supplementary Fig. 11D), though PI3K/AKT-FOXO-related genes were slightly induced (Supplementary Fig. 11E). Gene Set Enrichment Analysis of the transcriptome data revealed that tankyrase inhibitors negatively regulated MYC and E2F-related pathway genes (Fig. 5c and Supplementary Fig. 11F). Tankyrase inhibitors downregulated MYC protein in JC-11 but not in JC-494 cells (Fig. 5d). Downregulation of MYC signature gene expression after treatment with tankyrase inhibitors was also observed in wild-type *APC* JC-11 and JC-494 cells, while it was marginal in *APC*-mutated JC-21 and JC-475 cells (Suppl. Fig. 12A). *MYC* mRNA expression did not correlate with tankyrase inhibitor sensitivity in the *APC*-mutated CRC PDCs (Supplementary Fig. 12B, C).

We next examined E2F-related cell cycle regulators and found that RB phosphorylation at Ser-807/811 and cyclin D1 were decreased whereas p21 was upregulated upon treatment with tankyrase inhibitors in JC-11 cells (Fig. 5d). We also used three different *CDKN1A* (p21) siRNAs and found that #1 and #3 attenuated p21 induction by tankyrase inhibitors. These siRNAs partially counteracted the anti-proliferative effects of RK-582 on

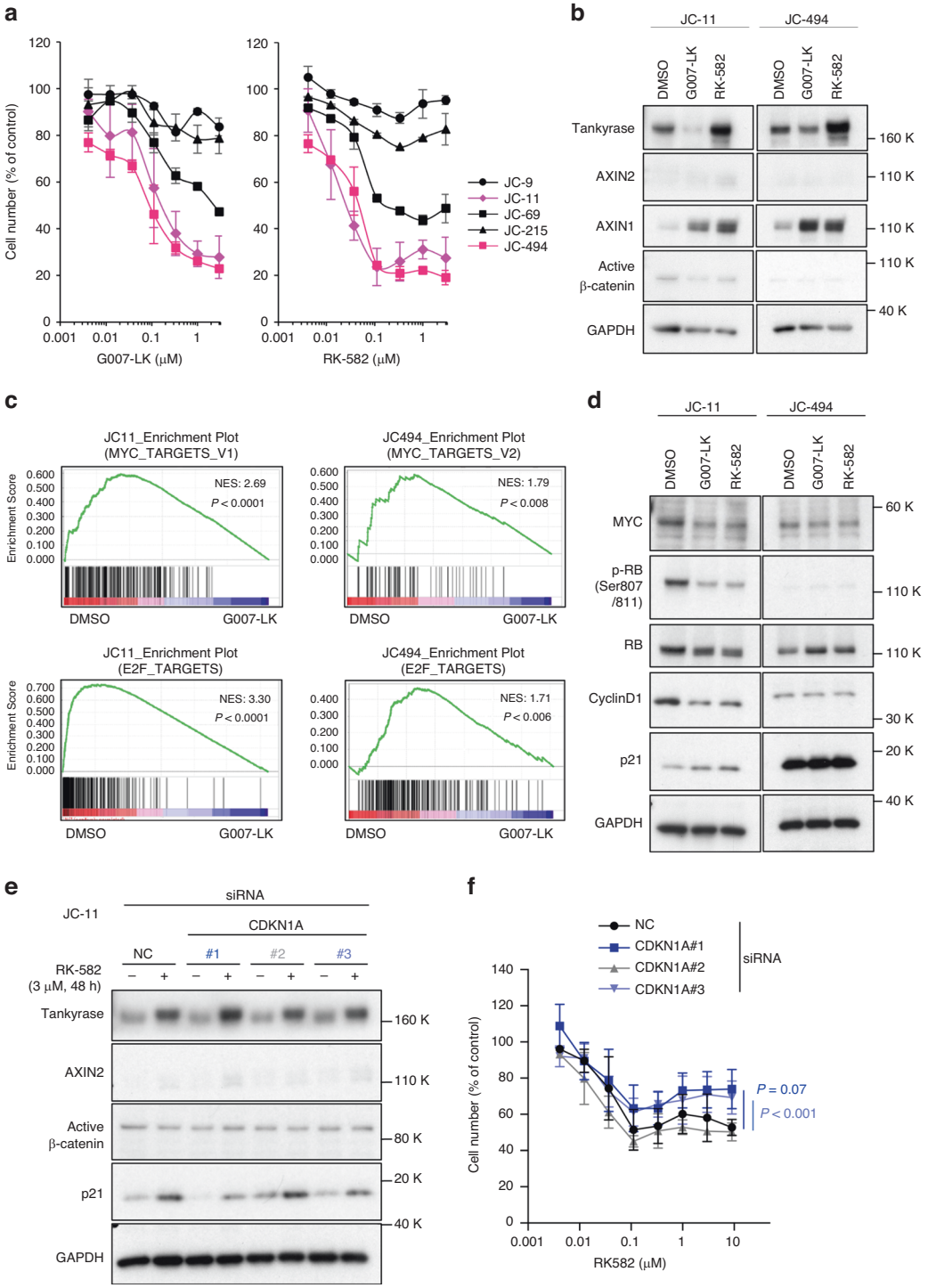

Fig. 5 Sensitivity of *APC*-wild CRC PDCs to tankyrase inhibitors and related molecular pathways. a Sensitivity of *APC*-wild PDCs to tankyrase inhibitors. Cell viability was determined after 5-day treatment with G007-LK and RK-582 in triplicate using MTT assay. Experiments were repeated at least twice, and the average values were plotted. *Error bar* indicates standard deviation. **b** Immunoblot analysis of tankyrase, AXINs, and β-catenin in JC-11 and JC-494 cells. Cells were treated with 0.3 μM G007-LK or RK-582 for 24 h. **c** Transcriptome analysis of G007-LK-treated PDCs. JC-11 and JC-494 cells were treated with 0.3 μM G007-LK for 24 h and subjected to GeneChip microarray analysis. Representative results of the Gene Set Enrichment Analysis are shown. NES: normalized enrichment score. **d** Immunoblot analysis of MYC and E2F1 pathway–related cell cycle regulators in JC-11 and JC-494 cells treated with 3 μM G007-LK or RK-582 for 24 h. **e** Knockdown of p21 (*CDKN1A*) by siRNAs in JC-11 cells. Cells were treated with p21/*CDKN1A* siRNAs (#1–3) or with negative control siRNA (NC) on day 0. After 24 h, RK-582 was added. Cells were collected on day 3, and knockdown efficacy was evaluated by immunoblot analysis. **f** Effect of p21/*CDKN1A* knockdown on the anti-proliferative effect of RK-582 in JC-11 cells. Cells were treated with siRNAs and RK-582 as in (**e**). Five days after the drug addition, relative cell number was quantitated by MTT assay. *Error bar* indicates standard deviation. For (**e**, **f**), experiments were performed three times, and reproducible results were obtained. For other data, experiments were performed at least twice, and reproducible results were obtained. Statistical significance was evaluated by repeated ANOVA using Microsoft Excel with Statcel 4 software.

JC-11 cells, although #1 did not show statistically significant difference with the control cells (Fig. 5e, f). These results indicate that tankyrase inhibitors suppress *APC*-wild CRC cell growth not through WNT, PI3/AKT, or YAP blockade but partially, at least, through inhibition of MYC- and E2F-related pathways.

DISCUSSION

Here we used an expanded cohort of CRC PDCs and confirmed that short *APC* mutations are a predictive biomarker of response to tankyrase inhibitors. Furthermore, active β-catenin may be an additional biomarker for the inhibitor-sensitive PDCs, even those with long *APC*. By contrast, tankyrase inhibitor–resistant PDCs frequently possessed *PIK3CA* mutations, which correlated with activated AKT. Given that β-catenin confers resistance to PI3K and AKT inhibitors in CRCs [37], WNT/β-catenin and PI3K-AKT pathways may share a compensational role in CRC cell survival and proliferation. We previously reported that acquired resistance of β-catenin-dependent CRC cells to tankyrase inhibitors involves activation of mTOR signaling, which is part of the PI3K-AKT pathway [31].

APC Min (multiple intestinal neoplasia) mouse has a mutant allele of *Apc* at codon 850 [38]. This model seems to be highly relevant and sensitive to tankyrase inhibition along with a conditional model (580 aa) [39]. By contrast, Schatoff et al. reported that such mutants do not respond to tankyrase inhibition [40]. They reported that CRC cells harboring *APC* mutations within the mutation cluster region, classified as the long *APC* mutations, were sensitive to tankyrase inhibitors [40]. In our present study with a larger number of clinically relevant CRC cells, 9 (out of 26) PDCs with *APC* mutations in the mutation cluster region were tankyrase inhibitor–resistant. This discrepancy could be in part attributed to difference in the cell contexts, including the culture conditions. Our results showed that tankyrase inhibitor–resistant PDCs with long *APC* mutations frequently activated AKT and were sensitive to BKM-120, a PI3K inhibitor. These observations suggest that these PDCs depend on PI3K-AKT rather than the β-catenin pathway.

The levels of active β-catenin are associated with the sensitivity to tankyrase inhibitors even in long *APC* type PDCs. We previously showed that long *APC* mutations are hypomorphic and the gene products partially retain the ability to downregulate β-catenin [21]. Intriguingly, even among the long *APC* type PDCs, the levels of active β-catenin significantly differed: *APC* truncation locations before approximately 1400 aa were associated with higher expression levels of active β-catenin. These observations suggest that complete or partial retainment of the "catenin inhibitory domain" between the second and third 20-AARs of APC (1404–1466 aa) contributes to the lower levels of active β-catenin. The levels of phosphorylated glycogen synthase kinase 3-β, which phosphorylates β-catenin for its ubiquitin-dependent degradation, did not correlate with those of active β-catenin (our unpublished observation). We also confirmed that PDCs used in the present study do not have driver or hotspot mutations in *CTNNB1*. Meanwhile, a gain-of-function mutant allele of *CTNNB1* (β-catenin lacking serine 45) confers resistance to tankyrase inhibitors [31].

Tankyrase inhibitor-sensitive cells showed (1) high dependence to β-catenin signaling, (2) short APC expression with highly active β-catenin, and (3) lack of *PIK3CA* mutation. In cancer cells, mutually exclusive activation of essential pathways is observed and each essential mutation status as well as dependence of cell proliferation on each pathway is closely related with each other. We speculate that the dependency of proliferation on the β-catenin pathway could be linked with the highly activated β-catenin status in the cells, which is caused by short APC mutation, and possibly coupled with less mutation in other related pathways such as *PIK3CA* mutation. In the APC mutant PDCs that we analyzed here, the level of APC protein expression could vary and the size of mainly expressed APC protein could not reflect the location of mutation in *APC* gene in several cells (Supplementary Fig. 3). This could be due to the heterogeneity of mutant *APC* expression in cancer cell population and to the possible difference of protein stability in each truncated APC protein.

The MEK-ERK pathway was activated in many PDCs regardless of their responsiveness to tankyrase inhibitors and *KRAS*/*BRAF* mutations (Supplementary Fig. 9A and Table 1). Tankyrase inhibition enhanced the antiproliferative effect of a MEK inhibitor on PDCs, consistent with previous reports [34, 41]. Mechanistically, we confirmed that MEK inhibition upregulated FGFR2 expression, which was abrogated by tankyrase inhibition in SW480 cells [34]. However, MEK inhibition did not upregulate FGFR2 in our PDCs, suggesting that other mechanisms contribute to the synergistic effect in these cells.

We observed so-called "bell-shaped" dose responses to tankyrase inhibitors in some PDCs (Fig. 1a). These phenomena have been reproducibly observed in fractions of sensitive and intermediate cells. Our preliminary results have indicated that higher doses of tankyrase inhibitors did not cause feedback activation of β-catenin in these cells. Instead, the cells elicited kinds of stress responses upon treatment with higher doses of the inhibitors (unpublished observations). Meanwhile, biomarkers that predict the cells with bell-shaped dose response remain to be determined.

In conclusion, *APC*/*PIK3CA* mutations and active β-catenin accumulation predict the efficacy of tankyrase inhibitors in CRC cells. Furthermore, some wild-type *APC* CRC cells were also sensitive to tankyrase inhibitors. Mechanistically, suppression of MYC and E2F-related pathways may be involved in the growth inhibition of wild-type *APC* cells. In fact, tankyrase PARsylates p21 and induces its degradation [42]. Consistently, we observed that tankyrase inhibition increases p21 protein level in wild-type *APC* cells. Since we and others are preparing for first-in-human clinical trials of tankyrase inhibitors, our present study will facilitate more precise patient selection in those clinical trials.

DATA AVAILABILITY

The gene expression data have been deposited in the Gene Expression Omnibus (accession numbers: GSE217758, GSE232209). Other data generated or analyzed during the current study are available from the corresponding author on reasonable request.

REFERENCES

1. Nielsen DL, Palshof JA, Larsen FO, Jensen BV, Pfeiffer P. A systematic review of salvage therapy to patients with metastatic colorectal cancer previously treated with fluorouracil, oxaliplatin and irinotecan +/− targeted therapy. Cancer Treat Rev. 2014;40:701–15.
2. Fodde R, Smits R, Clevers H. APC, signal transduction and genetic instability in colorectal cancer. Nat Rev Cancer. 2001;1:55–67.
3. Nishisho I, Nakamura Y, Miyoshi Y, Miki Y, Ando H, Horii A, et al. Mutations of chromosome 5q21 genes in FAP and colorectal cancer patients. Science 1991;253:665–9.
4. Daniloski Z, Bisht KK, McStay B, Smith S. Resolution of human ribosomal DNA occurs in anaphase, dependent on tankyrase 1, condensin II, and topoisomerase IIalpha. Genes Dev. 2019;33:276–81.
5. Ohishi T, Yoshida H, Katori M, Migita T, Muramatsu Y, Miyake M, et al. Tankyrase-binding protein TNKS1BP1 regulates actin cytoskeleton rearrangement and cancer cell invasion. Cancer Res. 2017;77:2328–38.
6. Smith S, Giriat I, Schmitt A, de Lange T. Tankyrase, a poly(ADP-ribose) polymerase at human telomeres. Science 1998;282:1484–7.
7. Callow MG, Tran H, Phu L, Lau T, Lee J, Sandoval WN, et al. Ubiquitin ligase RNF146 regulates tankyrase and Axin to promote Wnt signaling. PLoS One. 2011;6:e22595.

8. Huang SM, Mishina YM, Liu S, Cheung A, Stegmeier F, Michaud GA, et al. Tankyrase inhibition stabilizes axin and antagonizes Wnt signalling. Nature 2009;461:614–20.
9. Zhang Y, Liu S, Mickanin C, Feng Y, Charlat O, Michaud GA, et al. RNF146 is a poly(ADP-ribose)-directed E3 ligase that regulates axin degradation and Wnt signalling. Nat Cell Biol. 2011;13:623–9.
10. Riffell JL, Lord CJ, Ashworth A. Tankyrase-targeted therapeutics: expanding opportunities in the PARP family. Nat Rev Drug Discov. 2012;11:923–36.
11. Seimiya H. Crossroads of telomere biology and anticancer drug discovery. Cancer Sci. 2020;111:3089–99.
12. Chen B, Dodge ME, Tang W, Lu J, Ma Z, Fan CW, et al. Small molecule-mediated disruption of Wnt-dependent signaling in tissue regeneration and cancer. Nat Chem Biol. 2009;5:100–7.
13. Lau T, Chan E, Callow M, Waaler J, Boggs J, Blake RA, et al. A novel tankyrase small-molecule inhibitor suppresses APC mutation-driven colorectal tumor growth. Cancer Res. 2013;73:3132–44.
14. Quackenbush KS, Bagby S, Tai WM, Messersmith WA, Schreiber A, Greene J, et al. The novel tankyrase inhibitor (AZ1366) enhances irinotecan activity in tumors that exhibit elevated tankyrase and irinotecan resistance. Oncotarget 2016;7:28273–85.
15. Mizutani A, Yashiroda Y, Muramatsu Y, Yoshida H, Chikada T, Tsumura T, et al. RK-287107, a potent and specific tankyrase inhibitor, blocks colorectal cancer cell growth in a preclinical model. Cancer Sci. 2018;109:4003–14.
16. Shirai F, Mizutani A, Yashiroda Y, Tsumura T, Kano Y, Muramatsu Y, et al. Design and discovery of an orally efficacious spiroindolinone-based tankyrase inhibitor for the treatment of colon cancer. J Med Chem. 2020;63:4183–204.
17. Shirai F, Tsumura T, Yashiroda Y, Yuki H, Niwa H, Sato S, et al. Discovery of novel spiroindoline derivatives as selective tankyrase inhibitors. J Med Chem. 2019;62:3407–27.
18. Zhong Y, Katavolos P, Nguyen T, Lau T, Boggs J, Sambrone A, et al. Tankyrase inhibition causes reversible intestinal toxicity in mice with a therapeutic index <1. Toxicol Pathol. 2016;44:267–78.
19. Kim DY, Kwon YJ, Seo WY, Kim UI, Ahn S, Choi SM, et al. Tankyrase-selective inhibitor STP1002 shows preclinical antitumour efficacy without on-target toxicity in the gastrointestinal tract. Eur J Cancer. 2022;173:41–51.
20. Brinch SA, Amundsen-Isaksen E, Espada S, Hammarstrom C, Aizenshtadt A, Olsen PA, et al. The tankyrase inhibitor OM-153 demonstrates antitumor efficacy and a therapeutic window in mouse models. Cancer Res Commun. 2022;2:233–45.
21. Tanaka N, Mashima T, Mizutani A, Sato A, Aoyama A, Gong B, et al. APC mutations as a potential biomarker for sensitivity to tankyrase inhibitors in colorectal cancer. Mol Cancer Ther. 2017;16:752–62.
22. Jang MK, Mashima T, Seimiya H. Tankyrase inhibitors target colorectal cancer stem cells via AXIN-dependent downregulation of c-KIT tyrosine kinase. Mol Cancer Ther. 2020;19:765–76.
23. Bolger AM, Lohse M, Usadel B. Trimmomatic: a flexible trimmer for Illumina sequence data. Bioinformatics 2014;30:2114–20.
24. Li H. Aligning sequence reads, clone sequences and assembly contigs with BWA-MEM. arXiv 2013;1303:3997v2.
25. Li H, Handsaker B, Wysoker A, Fennell T, Ruan J, Homer N, et al. The sequence alignment/map format and SAMtools. Bioinformatics 2009;25:2078–9.
26. Cibulskis K, Lawrence MS, Carter SL, Sivachenko A, Jaffe D, Sougnez C, et al. Sensitive detection of somatic point mutations in impure and heterogeneous cancer samples. Nat Biotechnol. 2013;31:213–9.
27. McKenna A, Hanna M, Banks E, Sivachenko A, Cibulskis K, Kernytsky A, et al. The genome analysis toolkit: a MapReduce framework for analyzing next-generation DNA sequencing data. Genome Res. 2010;20:1297–303.
28. DePristo MA, Banks E, Poplin R, Garimella KV, Maguire JR, Hartl C, et al. A framework for variation discovery and genotyping using next-generation DNA sequencing data. Nat Genet. 2011;43:491–8.
29. Van der Auwera GA, Carneiro MO, Hartl C, Poplin R, Del Angel G, Levy-Moonshine A, et al. From FastQ data to high confidence variant calls: the Genome Analysis Toolkit best practices pipeline. Curr Protoc Bioinforma. 2013;43:11.10.1-11.10.33.
30. McLaren W, Gil L, Hunt SE, Riat HS, Ritchie GR, Thormann A, et al. The Ensembl Variant Effect Predictor. Genome Biol. 2016;17:122.
31. Mashima T, Taneda Y, Jang MK, Mizutani A, Muramatsu Y, Yoshida H, et al. mTOR signaling mediates resistance to tankyrase inhibitors in Wnt-driven colorectal cancer. Oncotarget 2017;8:47902–15.
32. Novak A, Dedhar S. Signaling through beta-catenin and Lef/Tcf. Cell Mol Life Sci. 1999;56:523–37.
33. Deng X, Hamamoto R, Vougiouklakis T, Wang R, Yoshioka Y, Suzuki T, et al. Critical roles of SMYD2-mediated beta-catenin methylation for nuclear translocation and activation of Wnt signaling. Oncotarget 2017;8:55837–47.
34. Schoumacher M, Hurov KE, Lehar J, Yan-Neale Y, Mishina Y, Sonkin D, et al. Inhibiting Tankyrases sensitizes KRAS-mutant cancer cells to MEK inhibitors via FGFR2 feedback signaling. Cancer Res. 2014;74:3294–305.
35. Mygland L, Brinch SA, Strand MF, Olsen PA, Aizenshtadt A, Lund K, et al. Identification of response signatures for tankyrase inhibitor treatment in tumor cell lines. iScience 2021;24:102807.
36. Wang Y, Xu X, Maglic D, Dill MT, Mojumdar K, Ng PK, et al. Comprehensive molecular characterization of the Hippo signaling pathway in cancer. Cell Rep. 2018;25:1304–17.e5.
37. Tenbaum SP, Ordonez-Moran P, Puig I, Chicote I, Arques O, Landolfi S, et al. beta-catenin confers resistance to PI3K and AKT inhibitors and subverts FOXO3a to promote metastasis in colon cancer. Nat Med. 2012;18:892–901.
38. Moser AR, Luongo C, Gould KA, McNeley MK, Shoemaker AR, Dove WF. ApcMin: a mouse model for intestinal and mammary tumorigenesis. Eur J Cancer. 1995;31A:1061–4.
39. Waaler J, Machon O, Tumova L, Dinh H, Korinek V, Wilson SR, et al. A novel tankyrase inhibitor decreases canonical Wnt signaling in colon carcinoma cells and reduces tumor growth in conditional APC mutant mice. Cancer Res. 2012;72:2822–32.
40. Schatoff EM, Goswami S, Zafra MP, Foronda M, Shusterman M, Leach BI, et al. Distinct colorectal cancer-associated APC mutations dictate response to tankyrase inhibition. Cancer Discov 2019;9:1358–71.
41. Solberg NT, Melheim M, Strand MF, Olsen PA, Krauss S. MEK inhibition induces canonical WNT signaling through YAP in KRAS mutated HCT-15 cells, and a cancer preventive FOXO3/FOXM1 ratio in combination with TNKS inhibition. Cancers (Basel). 2019;11:164.
42. Jung M, Kim W, Cho JW, Yang WH, Chung IK. Poly-ADP ribosylation of p21 by tankyrases promotes p21 degradation and regulates cell cycle progression. Biochem J. 2022;479:2379–94.

ACKNOWLEDGEMENTS

We thank Noritaka Tanaka, Yuki Shimizu, Bo Gong, Yuki Takahashi, Tomoko Oh-hara, Motoyoshi Iwakoshi, Shuhei Ishii, and Yuting Zhou for technical and experimental support and members of Seimiya laboratory for invaluable discussion. We thank Gabrielle White Wolf, PhD, from Edanz (https://jp.edanz.com/ac) for editing a draft of this manuscript.

AUTHOR CONTRIBUTIONS

MC, TM, TO: conceptualization, methodology, validation, formal analysis, investigation; writing original draft, review & editing, visualization. YM: methodology, validation, investigation, resources, writing original draft, review & editing, visualization. YS: software, investigation, resources, data curation, writing original draft. MT: validation, formal analysis, investigation, resources, writing original draft. NK, AN, SI, XY, M-KJ, AM: methodology, investigation. SM: methodology, validation, formal analysis, investigation, review & editing, visualization. KM: investigation, resources. MS: investigation, resources. AS: validation, investigation, visualization. HY: methodology, validation, investigation; visualization. KT: resources. KY: conceptualization, resources, review & editing. FS, SN: resources, review & editing. RK: conceptualization, investigation, resources, data curation, review & editing. HS: conceptualization, methodology, validation, formal analysis, investigation, resources, data curation, writing original draft, review & editing, visualization, supervision, project administration, funding acquisition. All the authors drafted or revised the manuscript, approved the final version, and agreed to be accountable for all aspects of the work in ensuring that questions related to the accuracy or integrity of any part of the work are appropriately investigated and resolved.

FUNDING

This work was supported by Grants-in-Aid for Scientific Research, Japan Society for the Promotion of Science [Scientific Research (B) 19H03523 and622H02931 to Hiroyuki Seimiya and Scientific Research (C) 18K07337 to Tetsuo Mashima], Project for Cancer Research and Therapeutic Evolution (167708578 to H. Seimiya), Practical Research for Innovative Cancer Control (19090105 and 22580621 to H. Seimiya), Project for Promotion of Cancer Research and Therapeutic Evolution (23810633 to T. Mashima), Japan Agency for Medical Research and Development, and grants from Nippon Foundation (to H. Seimiya) and Takeda Science Foundation (to H. Seimiya).

COMPETING INTERESTS

HS received research grants from the Nippon Foundation and Takeda Science Foundation and holds a patent of RK-582 and related chemical compounds. FS holds a patent of RK-582 and related chemical compounds. RK received a research grant from TOPPAN. The other authors declare no competing interests.

ETHICS APPROVAL AND CONSENT TO PARTICIPATE

This study was performed in accordance with the Declaration of Helsinki under approval from the Institutional Review Board of Japanese Foundation for Cancer Research (JFCR) (Tokyo, Japan) and the written informed consent of patients. Animal procedures were carried out, following national laws and policies (Guidelines for Proper Conduct of Animal Experiments, Science Council of Japan, 2006) in the animal experiment room at JFCR according to protocols approved by the JFCR Animal Care and Use Committee.

ADDITIONAL INFORMATION

Supplementary information The online version contains supplementary material available at https://doi.org/10.1038/s41416-023-02484-8.

Correspondence and requests for materials should be addressed to Hiroyuki Seimiya.

Reprints and permission information is available at http://www.nature.com/reprints

Publisher's note Springer Nature remains neutral with regard to jurisdictional claims in published maps and institutional affiliations.

Springer Nature or its licensor (e.g. a society or other partner) holds exclusive rights to this article under a publishing agreement with the author(s) or other rightsholder(s); author self-archiving of the accepted manuscript version of this article is solely governed by the terms of such publishing agreement and applicable law.